Differences in Transient Stability Between Grid Forming and Grid Following in Synchronization Mechanism

Ziqian Zhang[1], Robert Schürhuber[1], Lothar Fickert[1], Katrin Friedl[1], Guochu Chen[2], Yongming Zhang[2], Feng Wang[3]*

[1]*Graz University of Technology, Inffeldgasse 18, Graz, Austria*
[2]*Shanghai Dianji University, No. 300, Shuihua Road, Shanghai, China*
[3]*Xi'an Jiaotong University, No.28, Xianning West Road, Xi`an, China*
**ziqian.zhang@tugraz.at*

Keywords: Grid Forming, Grid Following, transient stability, phase portrait, domain of attraction

Abstract

As the share of inverters in the power system increases, the stability of inverters has an increasing impact on the reliable operation of power electronics dominated power systems. Since the synchronization mechanism plays a leading role in the dynamic performance of the inverter, its stability is one of the keys for the stable operation of the power system. The Grid Forming inverters have emerged in recent years, is completely different from the traditional Grid Following inverter in terms of synchronization mechanism. This paper will analyse and compare the differences in transient stability between the synchronization mechanisms of the two concepts of inverters through large-signal modelling and phase-portrait method. The analysis results show that the Grid Forming inverter is more robust in synchronization mechanism.

1. Introduction

At present, the inverters with the Grid Following concept still dominate in number. However, as different Grid Forming concepts are proposed and applied [1], affected by the different synchronization mechanism, the dynamic performance of power electronics dominated power systems becomes increasingly complex.

The Grid Forming inverter based on the concept of virtual synchronous generator [2] simulates the rotor equation of a synchronous generator in the synchronization algorithm. It can be equivalently regarded as a controlled voltage source. The output current of Grid Following inverter follows the grid frequency and phase angle obtained by the phase-locked loop. It can be equivalently regarded as a controlled current source [3]. The performance of the Grid Forming and Grid Following inverters are different during the voltage drop.

In this paper, the reduced-order large-signal modelling of the inverters with different synchronization mechanism are carried out in Section II and III, and its dynamic characteristics are described by nonlinear differential equations. Through the iterative solution of differential equations, this paper obtains the trajectories and domains of attraction in Section IV. Through the phase-portrait method, this paper analyzes the transient stability of different inverter during and after voltage drop.

2. Synchronization mechanism of inverter

2.1. Grid Forming inverter

A Grid Forming inverter with the concept of the virtual synchronous generator, similar to a synchronous generator, can be regarded as a controlled voltage source. The output voltage's phase angle is controlled by the active power-frequency loop (*P-f* loop), and the output voltage's amplitude is controlled by the reactive power-voltage amplitude loop (*Q-E* loop). As shown in Figure 1.

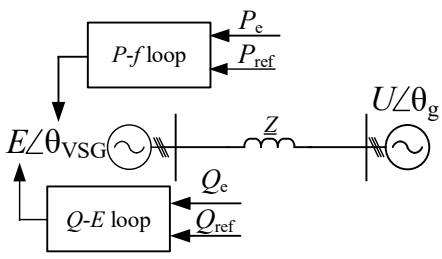

Fig. 1 Grid Forming inverter

A complete control block diagram of a typical Grid Forming inverter is shown in Figure 2 [4].

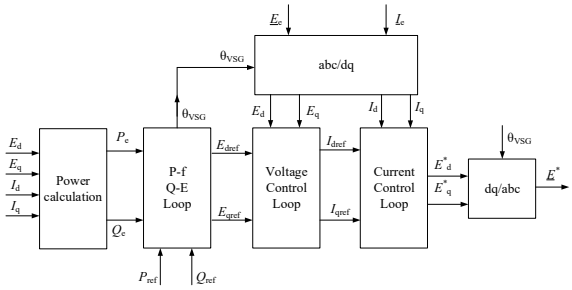

Fig.2 Control block diagram of a Grid Forming inverter

In the grid fault state, in order to prevent the output current amplitude from exceeding the threshold and damaging the power components, the output current amplitude is saturated [5]. The saturation on the output current amplitude is deployed in the voltage control unit. When the current reference exceeds the limit, which caused by a grid fault, the current reference by the voltage control unit is saturated. At this time, the *Q-E* loop and the voltage control unit no longer function. Only the *P-f* loop and the current control unit still operate effectively. Therefore, the Grid Forming inverter is converted from an equivalent controlled voltage source to an equivalent controlled current source, as shown in Figure 3.

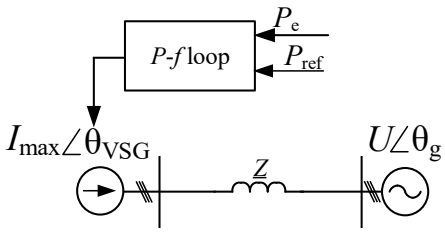

Fig.3 Grid Forming inverter in current source mode

2.2. Grid Following Inverter

A Grid Following inverter can be regarded as a controlled current source. The current phase angle is dominated by the phase-locked loop (PLL), and the current amplitude is controlled by the active power loop. As shown in Figure 4 [6].

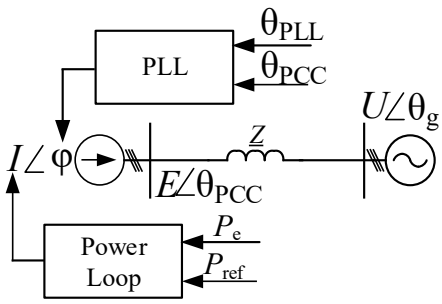

Fig.4 Grid Following inverter

A complete control block diagram of a typical Grid Following inverter is shown in Figure 5.
Since the Grid Following inverter originally operates in current source mode, even if the output current amplitude is saturated due to grid faults, it still operates in current source mode.

3. Mathematical modelling

In the cascade control system of Grid Forming and Grid Following inverters, the time constant of current and voltage control (~1 milliseconds) is much smaller than the time constant of synchronization mechanism (~100 milliseconds). The focus of this investigation is the stability of the inverter's synchronization mechanism, so in this paper, the current and voltage control loops are considered to be the ideal unit with unit gain.

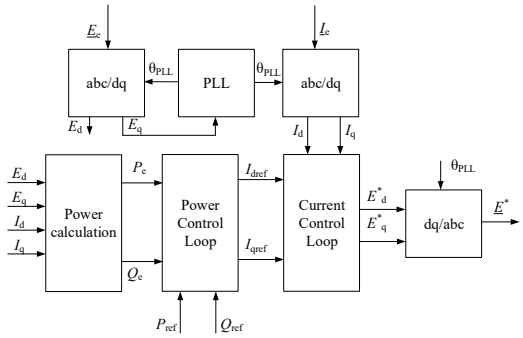

Fig.5 Control block diagram of a Grid Following inverter

In the time scale of this investigation, Gird Forming's *P-f* and *Q-E* loops are considered to be decoupled [7], so this paper only analyzes the influence of active power-frequency loop on the system.

3.1. Grid Forming Inverter

The Grid Forming inverter based on the virtual synchronous generator achieves synchronization with the grid voltage by using algorithms to imitate the rotor equation of a synchronous generator. A typical rotor equation of synchronous generator is expressed in (1).

$$\begin{cases} H\dfrac{d\Delta\omega(t)}{dt} = P_{\mathrm{ref}} - P_{\mathrm{e}} - D_{\mathrm{p}}\Delta\omega(t) \\ \dfrac{d\delta(t)}{dt} = \Delta\omega(t) \end{cases} \tag{1}$$

$\Delta\omega$ is the difference of angular frequency of synchronization mechanism and the grid voltage. H is the inertia coefficient and D_{p} is the damping coefficient. P_{e} is the active power output by the inverter, and P_{m} is the input power from virtual mechanical side, which will be replaced by P_{ref} here.
When considering the influence of the power grid on the inverter, the expression of P_{e} can be derived from Figure 1.

$$\begin{aligned} &P_{\mathrm{e}}\left(\delta(t)\right) \\ &= \frac{3}{2}\frac{1}{|Z|}\left(|E|^2\cos(\theta_Z) - |E||U|\cos\left(\theta_Z + \delta(t)\right)\right) \end{aligned} \tag{2}$$

Bring the (2) into the (1) to get a differential equation of a Grid Forming inverter (3).

$$\begin{aligned} &\frac{d^2}{dt^2}\delta(t) + \frac{D_{\mathrm{p}}}{H}\frac{d}{dt}\delta(t) - \frac{P_{\mathrm{ref}}}{H} + \\ &\frac{3}{2}\frac{1}{|Z|H}\left(|E|^2\cos(\theta_Z) - |E||U|\cos\left(\theta_Z + \delta(t)\right)\right) = 0 \end{aligned} \tag{3}$$

3.2. *Grid Forming Inverter with saturated current*

When a fault occurs and the output current of the inverter is saturated, the Grid Forming inverter is equivalent to a controlled current source. According to Figure 3, the expression of its active power output is now (4).

$$P_e\left(\delta(t)\right)=\frac{3}{2}\left|I_{\max}\right|\left|U\right|\cos\left(\delta(t)\right) \tag{4}$$

Bring the (4) into the (1) to get the differential equation of a Grid Forming inverter with saturated current (5).

$$\begin{aligned}&\frac{d^2}{dt^2}\delta(t)+\frac{D_p}{H}\frac{d}{dt}\delta(t)\\&-\frac{P_{ref}}{H}+\frac{3}{2}\frac{\left|I_{nax}\right|\left|U\right|}{H}\cos\left(\delta(t)\right)=0\end{aligned} \tag{5}$$

3.3. *Grid Following Inverter*

The synchronizer of the Grid Following inverter is a phase-locked loop. A typical synchronous reference frame- phase-locked loop (SRF-PLL) [8] is shown in Figure 6.

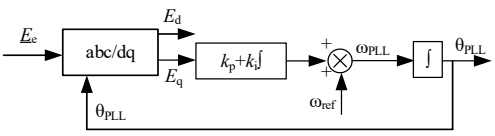

Fig.6 Control block of a SRF-PLL

A Grid Following inverter is regarded as a controlled current source. According to Figure 6, after dq-transformation, the q-axis component of the PCC voltage E_q is expressed in (6).

$$\begin{aligned}&E_q\left(\theta_{PLL}(t)\right)\\&=\left|Z\right|\left|I\right|\sin\left(\theta_Z+\theta_C\right)-\left|U\right|\sin\left(\theta_{PLL}(t)-\theta_g\right)\end{aligned} \tag{6}$$

Bring the (6) into the Figure 6 to get the differential equation of a Grid Following inverter (7).

$$\begin{aligned}&\frac{d^2}{dt^2}\theta_{PLL}(t)+k_p\left|U\right|\cos\left(\theta_{PLL}(t)-\theta_g\right)\frac{d}{dt}\theta_{PLL}(t)\\&+k_i\left|U\right|\sin\left(\theta_{PLL}(t)-\theta_g\right)-k_i\left|Z\right|\left|I\right|\sin\left(\theta_Z+\theta_C\right)=0\end{aligned} \tag{7}$$

4. Stability analysis

4.1. *Qualitative analysis of system operation's trajectory*

In order to quantify the difference in the stability of the synchronization mechanism between Grid Forming and Grid Following inverters, this section adopts the phase-portrait analysis method. A complete grid fault process can be divided into three stages, the first stage is pre-fault stage, the second stage is during the fault, and the third stage is after the fault is cleared.

The basic trajectories of the synchronization mechanism of the inverter is shown in Figure 7 [8].

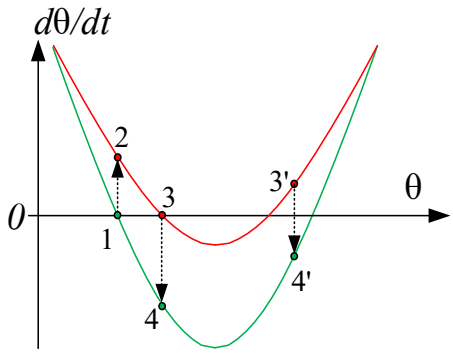

Fig.7 Basic trajectories of the synchronization mechanism of the inverter

In Figure 7, at first stage, when the grid is operating normally, the system's operating trajectory is a green curve. The operating point of the system stays at stable equilibrium point (SEP) 1. Its output phase angle θ is equal to its SEP, and its first differential term $d\theta/dt$ is equal to 0.

At the beginning of the second stage, due to changes in the grid state, the system's operating trajectory also changes, as shown in the red curve in Figure 7. Therefore, the system operating point jumps from the initial SEP 1 to point 2. The operating point starts to operate along the red trajectory. The initial operating point at this stage is 2, which means that the initial phase angle θ is the value at the SEP 1, but the initial value of the first-order differential term $d\theta/dt$ is not 0.

If there is still a SEP in the trajectory after grid fault, such as point 3 in Figure 7, then the operating point will move along the red trajectory from point 2 to 3, and finally stabilize at 3. At the moment when the grid fault is cleared, which is the 3rd stage, the system operating point changes from the trajectory during the fault (red curve) to the trajectory after the fault (green curve), the system operating point jumps from 3 to 4, and starts to operate along the green curve. The initial operating point at this stage is 3, which means that the initial phase angle θ is the value at the SEP 3, and the initial value of the first differential term $d\theta/dt$ is not 0.

If there is no SEP in the trajectory when the grid status changes, the system operating point continues to operate on the red trajectory until the fault is cleared. When the fault is cleared, the operating point jumps from 3' to 4' and operates along the green curve. The initial operating point at this stage is 3', which means that the initial phase angle θ is the value at 3', and the initial value of the first-order differential term $d\theta/dt$ is not 0.

When a fault occurs, and after the fault is cleared, the initial value of the first-order differential term is not zero. Therefore, these two moments are more likely to cause transient instability, but due to the short duration of the fault, the transient instability caused by the fault occurs will be reset by the changed grid state after the fault is cleared. After the fault is cleared, the grid state will remain unchanged, so the transient instability caused by the fault

clearing will continue. Therefore, the instability after the fault is cleared will cause more serious accidents. Therefore, this paper will investigate the system dynamics after the fault is cleared.

4.2. Quantitative analysis of system stability

In the quantitative phase-portrait analysis, we set the initial value of the nonlinear differential equations (3), (5) and (7) to its SEP plus the disturbance from grid fault. ϕ is the disturbance of the output phase angle $\delta(t)$ and $\theta_{\mathrm{PLL}}(t)$, and ε is the disturbance of the first differential term $d\delta(t)/dt$ and $d\theta_{\mathrm{PLL}}(t)/dt$. Then the nonlinear differential equations are solved iteratively by using the Runge–Kutta fourth-order method.

In order to distinguish each domains of attraction (DOA), the solution of the nonlinear differential equations when the time tends to infinity is marked on the phase plane as shown in Figure 8, Figure 9 and Figure 10 with different color blocks. The initial disturbance from grid fault are $\Phi = [-2\pi, 2\pi]$, $\varepsilon = [-45\pi, 45\pi]$. This paper applies approximate control time constants to the three types of inverters so that their results can be compared.

Figure 8 is DOA of the Grid Forming inverter based on the virtual synchronous generator when the current is not saturated.

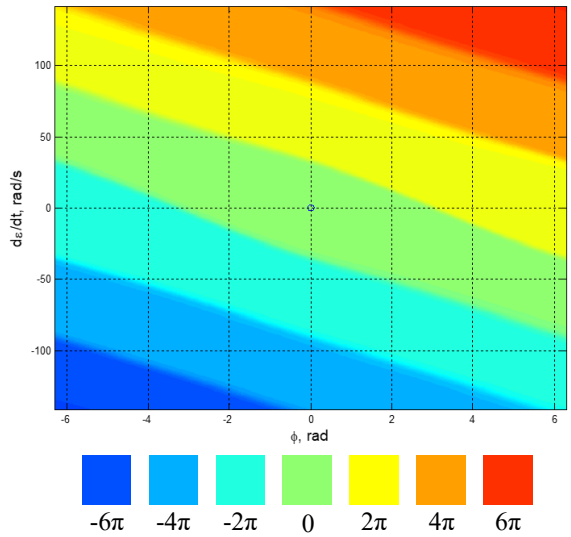

Fig.8 DOA of Grid Forming inverter

The color block in Figure 8 represents the position of the solution of the nonlinear differential equation (3) when time tends to infinity. The blue circle at the origin of the coordinates is the initial SEP, and the green area represents that the solution of the (3) in this area will gradually converge to the initial SEP. The solution in the yellow region will converge to the initial SEP+2π. The solution in the cyan region will converge to the initial SEP-2π, and so on.

When the system has a SEP during the fault, after the fault is cleared, the initial operating point of the system is on the line of $d\varepsilon/dt = 0$, and is generally located in the green area. Therefore, the system will eventually converge to the initial SEP.

When the system has no SEP during the fault, after the fault is cleared, the initial operating point of the system can be located at any area on the phase plane. And the longer the failure time lasts, the farther the operating point is from the initial SEP. Unlike a synchronous generator, an inverter has no physical rotating equipment. Therefore, the output angle of the Grid Forming inverter is not limited, and it can converge from any area. Therefore, the system can converge with any initial operating point.

Figure 9 is the DOA of the Grid Forming inverter based on the virtual synchronous generator when the current is saturated. Just like when the current is not saturated, the output angle can converge from any area.

In Figure 8, the DOA when the current is not saturated is symmetrically distributed around the initial SEP. Therefore, when a small disturbance from grid fault ends, the operating point of the system may still be in the green area, so the system is easier to converge to the initial SEP. In Figure 9, compared to Figure 8, the domains of attractive when the current is saturated has shifted by π to the left. This means that when a small disturbance from grid fault ends, the output phase angle will be easier to converge to the initial SEP + 2π.

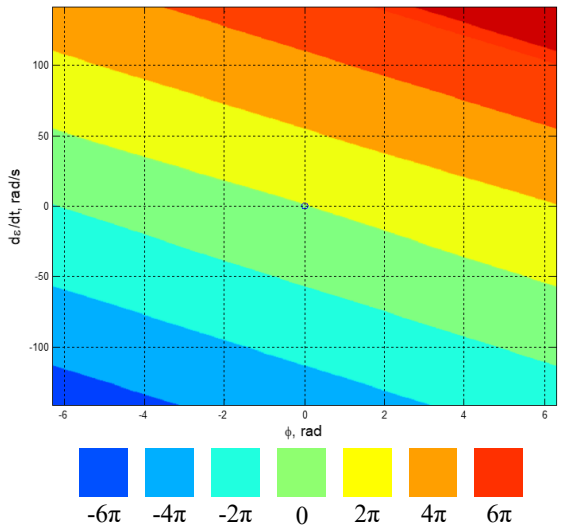

Fig.9 DOA of the Grid Forming inverter current is saturated

The cross-regional movement of the operating point of the synchronization mechanism after the end of the disturbance means a large change in the output phase angle, which causing errors in the dq transformation, which in turn leads to deviations in power control, voltage and current control. These deviations will cause the voltage or current in the system to exceed the limit and cause an accident.

In the domains of attraction of the Grid Following inverter in Figure 10, the initial operating points in some areas (dark brown areas) will cause the system to be unstable. Unlike the Grid Forming type inverter, the boundary of the DOA of the Grid Following inverter is not a straight line.

In addition, if the initial value of $d\varepsilon/dt$ is large, the solution of the Grid Forming inverter can also converge at other stable equilibrium points, but the solution of the Grid Following inverter with a PLL may diverge.

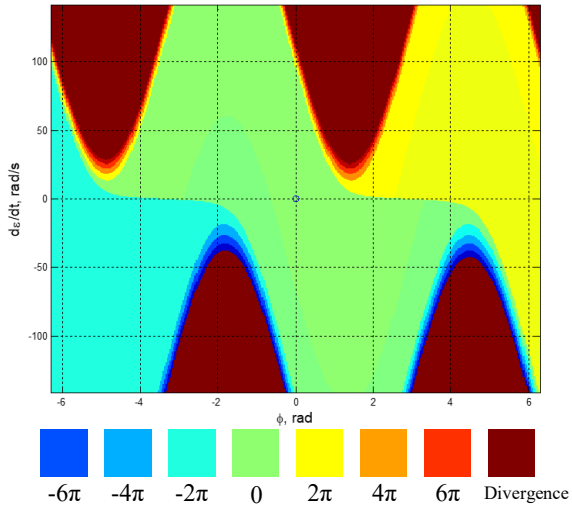

Fig.10 Domains of attraction of the Grid Following inverter

The divergence region in the phase plane exists periodically. When a fault occurs, if there is no SEP in the system, the operating point continues to be far away from the initial SEP. Its operating points may enter and leave multiple divergent areas (dark brown areas) one after another. When the operating point is located in a divergent area, and the fault is cleared, the system will not be able to operate stably after the fault is cleared. The multiple divergence areas cause the synchronization mechanism of Grid Following inverter to not have a fixed critical clearing time (CCT) point, but there are several critical clearing time ranges.

5. Conclusion

This paper analyzes the synchronization mechanism of Grid Forming inverter based on virtual synchronous generator and Grid Following inverter based on phase-locked loop. Aiming at the dynamic characteristics of its synchronization mechanism and the interaction of the power grid, this paper carries out the mathematical modelling for them. Based on the quadratic nonlinear differential equation, this paper analyzes its dynamic characteristics and stable performance in the phase plane.

There is no divergence area in the phase plane of the synchronization mechanism of the Grid Forming inverter based on the virtual synchronous generator. After the disturbance, the output phase angle can always return to a certain stable equilibrium point. For Grid Following inverter, there are multiple periodic divergence areas in the phase plane. After the fault is cleared, if the system operating point is located in the divergent area, the operating point will not be able to return to any stable equilibrium point, and the system will become unstable. Therefore, the robustness of the synchronization mechanism of the Grid Forming inverter based on the virtual synchronous generator is better than that of the Grid Following inverter based on the phase-locked loop when it encounters a grid fault.

6. References

[1] Poolla, B. K., Groß, D., & Dörfler, F. (2019). Placement and implementation of grid-forming and grid-following virtual inertia and fast frequency response. IEEE Transactions on Power Systems, 34(4), 3035-3046.

[2] Driesen, J., & Visscher, K. (2008, July). Virtual synchronous generators. In 2008 IEEE Power and Energy Society General Meeting-Conversion and Delivery of Electrical Energy in the 21st Century (pp. 1-3). IEEE.

[3] Sun, J. (2011). Impedance-based stability criterion for grid-connected inverters. IEEE transactions on power electronics, 26(11), 3075-3078.

[4] Vinayagam, A., Swarna, K. S. V., Khoo, S. Y., Oo, A. T., & Stojcevski, A. (2017). PV based microgrid with grid-support grid-forming inverter control-(simulation and analysis). Smart grid and renewable energy, 8(01), 1-30.

[5] Taul, M. G., Wang, X., Davari, P., & Blaabjerg, F. (2019). Current limiting control with enhanced dynamics of grid-forming converters during fault conditions. IEEE Journal of Emerging and Selected Topics in Power Electronics, 8(2), 1062-1073.

[6] Zhang, Z., Gercek, C., Renner, H., Reinders, A., & Fickert, L. (2019). Resonance instability of photovoltaic E-bike charging stations: Control parameters analysis, modeling and experiment. Applied Sciences, 9(2), 252.

[7] Wu, H., Ruan, X., Yang, D., Chen, X., Zhao, W., Lv, Z., & Zhong, Q. C. (2016). Small-signal modeling and parameters design for virtual synchronous generators. IEEE Transactions on Industrial Electronics, 63(7), 4292-4303.

[8] Zhang, Z., Schürhuber, R., Fickert, L., & Zhang, Y. (2018, October). Stability of Grid-connected Photovoltaic Inverters During and After Low Voltage Ride Through. In 8th Solar Integration Workshop: International Workshop on Integration of Solar into Power Systems.